The 2009 IEEE/RSJ International Conference on
Intelligent Robots and Systems
October 11-15, 2009 St. Louis, USA

Dynamic Grasping for an Arbitrary Polyhedral Object by a Multi-Fingered Hand-Arm System

Akihiro Kawamura, Kenji Tahara, Ryo Kurazume and Tsutomu Hasegawa

Abstract— **This paper proposes a novel control method for stable grasping using a multi-fingered hand-arm system with soft hemispherical finger tips. The proposed method is simple but easily achieves stable grasping of an arbitrary polyhedral object using an arbitrary number of fingers. Firstly, we formulate nonholonomic constraints between a multi-fingered hand-arm system and an object constrained by rolling contact with finger tips, and derive a condition for stable grasping by stability analysis. A new index for evaluating the possibility of stable grasping is proposed and efficient initial relative positions between finger tips and the object for realizing stable grasping are analyzed. The stability of the proposed system and the validity of the index are verified through numerical simulations.**

I. Introduction

A multi-fingered hand-arm system has been expected to realize dexterous grasping like a human hand. Robots with this system will be able to perform various manipulation tasks even in an unstructured environment safely. Many robotics systems and control methods for grasping an object with an arbitrary shape have been proposed [1–5]. Especially, dynamic grasping controllers using rolling constraints have been reported [6–9]. However, these controllers are based on inverse dynamics calculation, and object information such as the mass and the shape of the object is required. In contrast, there are several researches for dynamic grasping of an unknown object using external sensing devices such as a vision sensor and a tactile sensor [10–12]. In these methods, sensing devices are costly and sensing error must be taken into consideration though object information is not required in advance.

On the other hand, Wimböck *et al.* [13] proposed a dynamic grasping method for an arbitrary object which requires neither object information nor external sensors. However, the stability of the system and the convergence performance of the closed-loop dynamics were not discussed. Moreover, rolling constraints between fingertips and the object surfaces are not considered in their method. Similarly, Arimoto *et al.* [14–17] have proposed a dynamic object grasping method without object information and external sensors. The object is limited to the one which consists of two flat and parallel surfaces, though they verified the stability of the system and the convergent performance of the closed-loop dynamics.

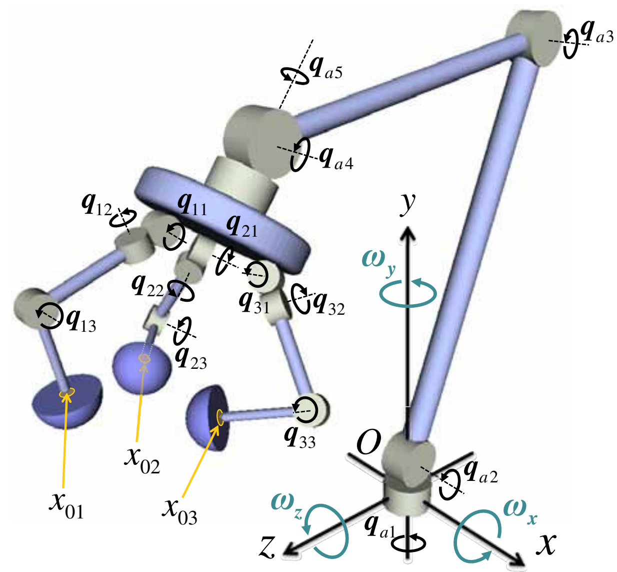

Fig. 1. Multi-fingered hand-arm system

This paper proposes a novel control method for stable grasping of an arbitrary polyhedral object using a multi-fingered hand-arm system with soft hemispherical finger tips. The proposed method is simple but easily achieves stable grasping of an object without use of preliminary information for a grasped object and any external sensors using an arbitrary number of fingers. Firstly, we formulate nonholonomic constraints between a multi-fingered hand-arm system and an object constrained by rolling contact with finger tips. The nonholonomic constraints for rolling contact were proposed by Arimoto *et al.* [14–17] for an object with two flat and parallel surfaces. We expand these constraints for an object with an arbitrary polyhedral shape. The number of fingers is also variable in our formulation. Secondly, we derive Lagrange's equation of motion for a hand-arm system, and propose a new control signal which achieves stable grasping. A new index for evaluating the possibility of stable grasping is proposed and efficient initial relative positions between finger tips and an object for realizing stable grasping are analyzed. Using this index, it is clarified that appropriate initial positions of finger tips depend on the shape of the object and the ratio of the size of the object and the radius of the finger tip. The stability of the proposed system and the validity of the index are verified through numerical simulations.

This work was partially supported by "the Kyushu University Research Superstar Program (SSP)", based on the budget of Kyushu University allocated under President's initiative.

A. Kawamura is with the Graduate School of Information Science and Electrical Engineering, Kyushu University, Fukuoka, 819-0395, JAPAN kawamura@irvs.is.kyushu-u.ac.jp

K. Tahara is with the Organization for the Promotion of Advanced Research, Kyushu University, Fukuoka, 819-0395, JAPAN tahara@ieee.org

R. Kurazume and T. Hasegawa are with the Faculty of Information Science and Electrical Engineering, Kyushu University, Fukuoka, JAPAN {kurazume, hasegawa}@ait.kyushu-u.ac.jp

978-1-4244-3804-4/09/$25.00 ©2009 IEEE

II. A Multi Fingered Hand Arm System

In this section, we define a model of a hand-arm system composed of an arm and a multi-fingered hand. An example of a multi-fingered hand-arm system treated here is illustrated in Fig. 1. An object to be grasped is an arbitrary polyhedral object whose surfaces touched by finger tips are flat. All finger tips maintain rolling contact with the object surfaces, and do not slip and detach from the surfaces during movement of the tips. Assume that fingertips roll within the ranges of hemisphere surfaces, and they don't deviate from each contact surface. Note that the gravity effect is ignored in this paper in order to have a physical insight into analyzing physical interaction and stability of the system. As shown in Fig. 1, O denotes the origin of Cartesian coordinates. $\boldsymbol{x}_{0i} \in \mathbb{R}^3$ is the center of each contact area. Hereafter, the subscript of i refers to the ith finger in all equations. The degrees of freedom of the arm and the ith finger are N_a and N_i, respectively. The joint angle of the arm is expressed by $\boldsymbol{q}_a \in \mathbb{R}^{N_a}$. Similarly, the joint angle of the ith finger is expressed by $\boldsymbol{q}_{0i} \in \mathbb{R}^{\mathrm{N}_i}$. $\boldsymbol{q}$ denotes the joint angles of the arm and all the fingers $\left(= (\boldsymbol{q}_a, \boldsymbol{q}_{01}, \boldsymbol{q}_{02}, ..., \boldsymbol{q}_{0N})^{\mathrm{T}}\right)$. N is the number of the fingers. As shown in Fig. 2, $O_{c.m.}$ denotes the center of the object mass and the origin of local coordinates. Its position in Cartesian coordinates is expressed as $\boldsymbol{x} = (x, y, z)^{\mathrm{T}} \in \mathbb{R}^3$. Instantaneous rotational axis of the object at $O_{c.m.}$ is expressed by $\boldsymbol{\omega}$. The orientation angular velocities around each axis of Cartesian coordinates x, y, z are expressed as $\omega_x, \omega_y, \omega_z$ respectively.

A. Constraints

3-dimentional rolling constraints with area contacts are modeled here. The orientation of the object in Cartesian coordinates can be expressed by the rotational matrix $\boldsymbol{R}$ such that

$$\boldsymbol{R}_{ob} = (\boldsymbol{r}_X, \boldsymbol{r}_Y, \boldsymbol{r}_Z) \in SO(3), \tag{1}$$

where $\boldsymbol{r}_X, \boldsymbol{r}_Y, \boldsymbol{r}_Z \in \mathbb{R}^3$ are mutually orthonormal vectors on the object frame. It is known that this rotational matrix is one of the members of the group $SO(3)$. In addition to this, we define contact frames at the center of each contact area as follows:

$$\boldsymbol{R}_{ob}\boldsymbol{R}_{Ci} = (\boldsymbol{C}_{iX}, \boldsymbol{C}_{iY}, \boldsymbol{C}_{iZ}), \tag{2}$$

where $\boldsymbol{R}_{Ci}$ is the rotational matrix between the object frame to the contact frames. Now, we consider the velocity of the center of the contact area $\boldsymbol{v}_i$ must satisfy

$$\boldsymbol{v}_i = \Delta r_i \left(\dot{\boldsymbol{C}}_{iY} - \boldsymbol{\omega}_i \times \boldsymbol{C}_{iY}\right), \tag{3}$$

where $\boldsymbol{\omega}_i \in \mathbb{R}^3$ is the orientation angular velocity vectors for each robotic finger on the contact frames, r_i is the radius of each finger tip, and Δr_i are the distance between the center of the finger tips and the contact surfaces (see Fig. 2). $\boldsymbol{v}_i$ is on the tangential plane at the center of the contact area (now, they are surfaces of the object). The rolling constraints

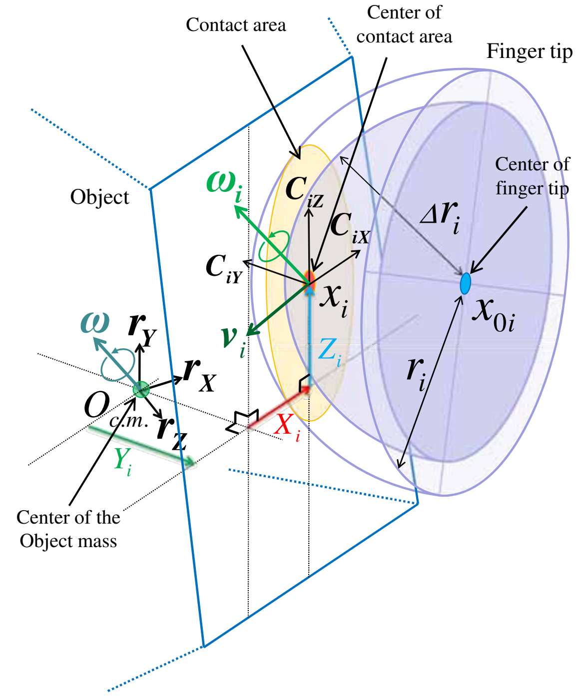

Fig. 2. Contact model at the center of the contact area

are expressed such that the velocity of the center of the contact area on the finger tip, given as (3), should equal to the velocity of the center of the contact area on the object surface

$$\Delta r_i \boldsymbol{C}_{iX}^{\mathrm{T}} \left(\dot{\boldsymbol{C}}_{iY} - \boldsymbol{\omega}_i \times \boldsymbol{C}_{iY}\right) = \dot{X}_i \tag{4}$$

$$\Delta r_i \boldsymbol{C}_{iZ}^{\mathrm{T}} \left(\dot{\boldsymbol{C}}_{iY} - \boldsymbol{\omega}_i \times \boldsymbol{C}_{iY}\right) = \dot{Z}_i, \tag{5}$$

where

$$X_i = -\boldsymbol{C}_{iX}^{\mathrm{T}}(\boldsymbol{x} - \boldsymbol{x}_{0i}) \tag{6}$$

$$Z_i = -\boldsymbol{C}_{iZ}^{\mathrm{T}}(\boldsymbol{x} - \boldsymbol{x}_{0i}). \tag{7}$$

Equations (4) and (5) denote nonholonomic rolling constraints on the object surfaces. These constrains are of linear with respect to each velocity vector, and thereby they can be expressed as Pfaffian constraints as follows:

$$\boldsymbol{X}_{iq}\dot{\boldsymbol{q}} + \boldsymbol{X}_{ix}\dot{\boldsymbol{x}} + \boldsymbol{X}_{i\omega}\boldsymbol{\omega} = 0 \tag{8}$$

$$\boldsymbol{Z}_{iq}\dot{\boldsymbol{q}} + \boldsymbol{Z}_{ix}\dot{\boldsymbol{x}} + \boldsymbol{Z}_{i\omega}\boldsymbol{\omega} = 0, \tag{9}$$

where

$$\left[\begin{array}{l} \boldsymbol{X}_{iq} = \Delta r_i \boldsymbol{C}_{iZ}^{\mathrm{T}} \boldsymbol{J}_{\Omega i} - \boldsymbol{C}_{iX}^{\mathrm{T}} \boldsymbol{J}_{0i} \\ \boldsymbol{X}_{ix} = \boldsymbol{C}_{iX}^{\mathrm{T}} \\ \boldsymbol{X}_{i\omega} = \{\boldsymbol{C}_{iX} \times (\boldsymbol{x} - \boldsymbol{x}_{0i})\}^{\mathrm{T}} - \Delta r_i \boldsymbol{C}_{iZ}^{\mathrm{T}} \\ \boldsymbol{Z}_{iq} = -\Delta r_i \boldsymbol{C}_{iX}^{\mathrm{T}} \boldsymbol{J}_{\Omega i} - \boldsymbol{C}_{iZ}^{\mathrm{T}} \boldsymbol{J}_{0i} \\ \boldsymbol{Z}_{ix} = \boldsymbol{C}_{iZ}^{\mathrm{T}} \\ \boldsymbol{Z}_{i\omega} = \{\boldsymbol{C}_{iZ} \times (\boldsymbol{x} - \boldsymbol{x}_{0i})\}^{\mathrm{T}} + \Delta r_i \boldsymbol{C}_{iX}^{\mathrm{T}}, \end{array}\right. \tag{10}$$

and $\boldsymbol{\omega} = (\omega_x, \omega_y, \omega_z)^{\mathrm{T}} \in \mathbb{R}^3$ is the angular velocity vector for the instantaneous rotational axis of the object. $\boldsymbol{J}_{\Omega_i} \in \mathbb{R}^{3\times\left(N_a + \sum_{i=1}^{N} N_i\right)}$ is the Jacobian matrix for the orientation angular velocities of the finger tips with respect to the joint angular velocity $\dot{\boldsymbol{q}} \in \mathbb{R}^{N_a+\sum_{i=1}^{N} N_i}$. $\boldsymbol{J}_{0i} \in \mathbb{R}^{3\times\left(N_a+\sum_{i=1}^{N} N_i\right)}$ is the Jacobian matrix for the center of the finger tip $\boldsymbol{x}_{0i}$ with respect to the joint angle, respectively.

B. Contact Model of Soft Finger-Tip

In this paper, the physical relationship between the deformation of the finger tip at the center of the contact area and its reproducing force is given on the basis of lumped-parameterized model proposed by Arimoto *et al* [14]. The reproducing force $f(\Delta r)$ in the normal direction to the object surface at the center of the contact area is given as follows:

$$\left[\begin{array}{l} f_i = \bar{f}_i + \xi_i \frac{d}{dt}(r_i - \Delta r_i) \\ \bar{f}_i = k(r_i - \Delta r_i)^2, \end{array}\right. \tag{11}$$

where k is a positive stiffness constant which depends on the material of the finger tip. In the second term of the right-hand side of the upper equation of (11), $\xi_i(\Delta r_i)$ is a positive scalar function with respect to Δr_i, and thereby the viscous force increases according to the expansion of the contact area.

C. Overall Dynamics

The total kinetic energy for the overall system can be described as follows:

$$K = \frac{1}{2}\dot{\boldsymbol{q}}^{\mathrm{T}}\boldsymbol{H}\dot{\boldsymbol{q}} + \frac{1}{2}\dot{\boldsymbol{x}}^{\mathrm{T}}\boldsymbol{M}\dot{\boldsymbol{x}} + \frac{1}{2}\boldsymbol{\omega}^{\mathrm{T}}\boldsymbol{I}\boldsymbol{\omega}, \tag{12}$$

where $\boldsymbol{H} \in \mathbb{R}^{\left(N_a+\sum_{i=1}^{N} N_i\right)\times\left(N_a+\sum_{i=1}^{N} N_i\right)}$ is the inertia matrix for the arm and the fingers, $\boldsymbol{M} = \mathrm{diag}(m,m,m)$ is the mass of the object, $\boldsymbol{I} = \boldsymbol{R}\bar{\boldsymbol{I}}\boldsymbol{R}^{\mathrm{T}}$ and $\bar{\boldsymbol{I}} \in \mathbb{R}^{3\times3}$ are the inertia tensors for the object represented by the principal axes of inertia. On the other hand, the total potential energy for the overall system is given as follows:

$$P = \sum_{i=1}^{N} P(\Delta r_i) = \sum_{i=1}^{N} \int_0^{r_i-\Delta r_i} \bar{f}_i(\Delta r_i)\, d\zeta, \tag{13}$$

where $P(\Delta r_i)$ is the elastic potential energy for each finger generated by the deformation of the finger tip. Hence, Lagrange's equation of motion is expressed by applying the variational principle as follows:

For the multi-fingered hand-arm system:

$$\boldsymbol{H}(\boldsymbol{q})\ddot{\boldsymbol{q}} + \left\{\frac{1}{2}\dot{\boldsymbol{H}}(\boldsymbol{q}) + \boldsymbol{S}(\boldsymbol{q},\dot{\boldsymbol{q}})\right\}\dot{\boldsymbol{q}} + \sum_{i=1}^{N}\left(\boldsymbol{J}_{0i}^{\mathrm{T}}\boldsymbol{C}_{iY} f_i + \boldsymbol{X}_{iq}^{\mathrm{T}}\lambda_{iX} + \boldsymbol{Z}_{iq}^{\mathrm{T}}\lambda_{iZ}\right) = \boldsymbol{u}, \tag{14}$$

For the object:

$$\boldsymbol{M}\ddot{\boldsymbol{x}} + \sum_{i=1}^{N}\left(-f_i\boldsymbol{C}_{iY} + \boldsymbol{X}_{ix}^{\mathrm{T}}\lambda_{iX} + \boldsymbol{Z}_{ix}^{\mathrm{T}}\lambda_{iZ}\right) = 0 \tag{15}$$

$$\boldsymbol{I}\dot{\boldsymbol{\omega}} + \left\{\frac{1}{2}\dot{\boldsymbol{I}} + \boldsymbol{S}\right\}\boldsymbol{\omega} - \sum_{i=1}^{N}\{\boldsymbol{C}_{iY}\times(\boldsymbol{x}-\boldsymbol{x}_{0i})\}f_i + \sum_{i=1}^{N}\left(\boldsymbol{X}_{i\omega}^{\mathrm{T}}\lambda_{iX} + \boldsymbol{Z}_{i\omega}^{\mathrm{T}}\lambda_{iZ}\right) = 0, \tag{16}$$

where $\boldsymbol{S}(\boldsymbol{q},\dot{\boldsymbol{q}})$ is skew-symmetric matrix, $\boldsymbol{u}$ is a vector of the input torque. In addition, λ_{iX} and λ_{iZ} denote Lagrange's multipliers.

III. CONTROL INPUT

Tahara *et al.* [17] proposed a simple control method of a triple robotic fingers system for stable grasping. We propose a new control method based on Tahara's method for a multi fingered hand-arm system. This control signal is designed so that the center of each finger tip approaches each other. The control signal is given as follows:

$$\boldsymbol{u} = \frac{f_d}{\sum_{i=1}^{N} r_i}\sum_{j=1}^{N}\boldsymbol{J}_{0j}(\boldsymbol{x}_d - \boldsymbol{x}_{0j}) - \boldsymbol{C}\dot{\boldsymbol{q}} \tag{17}$$

$$\boldsymbol{x}_d = \frac{1}{N}\sum_{i=1}^{N}\boldsymbol{x}_{0i}, \tag{18}$$

where $\boldsymbol{C} \in \mathbb{R}^{\left(N_a+\sum_{i=1}^{N} N_i\right)\times\left(N_a+\sum_{i=1}^{N} N_i\right)} > 0$ is a diagonal positive definite matrix that expresses the damping gain for each finger, and f_d is the nominal desired grasping force. Now, an output vector of overall system is given as follows:

$$\dot{\Lambda} = (\dot{\boldsymbol{q}}, \dot{\boldsymbol{x}}, \boldsymbol{\omega})^{\mathrm{T}}. \tag{19}$$

By substituting (17) into (14) and taking a sum of inner product of (19) and closed loop dynamics expressed by (14), (15) and (16), we obtain

$$\frac{d}{dt}E = -\dot{\boldsymbol{q}}^{\mathrm{T}}\boldsymbol{C}\dot{\boldsymbol{q}} - \sum_{i=1}^{N}\xi\Delta\dot{r}_i^2 \le 0 \tag{20}$$

$$E = K + V + \Delta P \ge 0 \tag{21}$$

$$K = \frac{1}{2}\dot{\boldsymbol{q}}^{\mathrm{T}}\boldsymbol{H}\dot{\boldsymbol{q}} + \frac{1}{2}\dot{\boldsymbol{x}}^{\mathrm{T}}\boldsymbol{M}\dot{\boldsymbol{x}} + \frac{1}{2}\boldsymbol{\omega}^{\mathrm{T}}\boldsymbol{I}\boldsymbol{\omega} \tag{22}$$

$$V = \frac{A}{2}\Big\{(\boldsymbol{x}_{01}-\boldsymbol{x}_{02})^2 + (\boldsymbol{x}_{02}-\boldsymbol{x}_{03})^2 + \dots + (\boldsymbol{x}_{0N}-\boldsymbol{x}_{01})^2\Big\} \tag{23}$$

$$\Delta P = \sum_{i=1}^{N}\int_0^{\delta r_i}\left\{\bar{f}_i(\Delta r_{di}+\phi) - \bar{f}_i(\Delta r_{di})\right\}d\phi, \tag{24}$$

where

$$\delta r_i = \Delta r_{di} - \Delta r_i \tag{25}$$

$$A = \frac{f_d}{N\left(\sum_{i=1}^{N} r_i\right)}. \tag{26}$$

Δr_{di} is an initial value of Δr_i. V plays a roll of an artificial potential energy arisen from the control input. Equation (21) is evident since K, V and ΔP are positive as far as $0 \le \Delta r_{di} - \delta r_i < r_i$. In addition, $\dot{E} \le 0$ during movement. Equations (20) and (21) yield

$$\int_0^{\infty}\left(\dot{\boldsymbol{q}}^{\mathrm{T}}\boldsymbol{C}\dot{\boldsymbol{q}} + \sum_{i=1}^{N}\xi\Delta\dot{r}_i^2\right)dt \le E(0) - E(t) \le E(0), \tag{27}$$

Equation (27) shows that the joint angular velocity $\dot{\boldsymbol{q}}(t)$ is squared integrable over time $t \in [0,\infty)$. It shows that $\dot{\boldsymbol{q}}(t) \in$

$L^2(0,\infty)$. Considering the constraints shown by (4) and (5), it is clear that $\dot{\boldsymbol{x}} \in L^2(0,\infty)$ and $\boldsymbol{\omega} \in L^2(0,\infty)$. Thereby, the output of the overall system $\dot{\Lambda}(t)$ is uniformly continuous since it is shown that $\dot{\Lambda} \to 0$ and $\ddot{\Lambda} \to 0$ when $t \to \infty$ [15]. Therefore, it is obvious that the sum of the external force applied to the finger system and the object $\boldsymbol{\Delta}\lambda_\infty$ is converged to zero.

$$\boldsymbol{\Delta}\lambda_\infty = (\boldsymbol{\Delta}\lambda_{\boldsymbol{q}}, \boldsymbol{\Delta}\lambda_{\boldsymbol{x}}, \boldsymbol{\Delta}\lambda_{\boldsymbol{\omega}}) \to 0 \tag{28}$$

where

$$\boldsymbol{\Delta}\lambda_{\boldsymbol{q}} = \sum_{i=1}^{N}\Big(\boldsymbol{J}_{0i}^{\mathrm{T}}\boldsymbol{C}_{iY}f_i + \boldsymbol{X}_{iq}^{\mathrm{T}}\boldsymbol{\lambda}_{iX} + \boldsymbol{Z}_{iq}^{\mathrm{T}}\boldsymbol{\lambda}_{iZ}\Big) - \boldsymbol{u} \tag{29}$$

$$\boldsymbol{\Delta}\lambda_{\boldsymbol{x}} = \sum_{i=1}^{N}\Big(-f_i\boldsymbol{C}_{iY} + \boldsymbol{X}_{ix}^{\mathrm{T}}\boldsymbol{\lambda}_{iX} + \boldsymbol{Z}_{ix}^{\mathrm{T}}\boldsymbol{\lambda}_{iZ}\Big) \tag{30}$$

$$\boldsymbol{\Delta}\lambda_{\boldsymbol{\omega}} = -\sum_{i=1}^{N}\{\boldsymbol{C}_{iY} \times (\boldsymbol{x} - \boldsymbol{x}_{0i})\}f_i + \sum_{i=1}^{N}\Big(\boldsymbol{X}_{i\omega}^{\mathrm{T}}\boldsymbol{\lambda}_{iX} + \boldsymbol{Z}_{i\omega}^{\mathrm{T}}\boldsymbol{\lambda}_{iZ}\Big). \tag{31}$$

As a consequence, it is shown the dynamic force/torque equibilium condition for immobilization of the object is satisfied since each external force and each velocity become zero. In other words, the stability of the overall systems is verified. However, it is necessary to consider the stability from physical perspective since the stability is analyzed only from a mathmatical viewpoint. There are some cases that one of the centers of the contact areas is outside of the object surfaces at the final state. Therefore, there is a requirement to specify the shape of the object to argue the stability from physical perspective. Moreover we argue a final state of the overall system mainly, because an overall movement depends on each damping gain and initial contact position but it is not depended on the final state of the system. Thereby in this paper, we focus on a final state of the overall system as the initial step of convergence analysis. Of course, it is important to consider the convergence of overall movement and it is one of our next works.

In the next section, as an example, we introduce the condition for an object with an arbitrary polygonal shape.

IV. Specific Study

In this section, the condition for stable grasping of an arbitrary polyhedral object is shown. In addition, an example of the condition for a triangle pole is introduced.

The final positions of the finger tips are obtained when E is minimized. On the other hand, the positions of the finger tips when E is minimized ($= E_{\min}$) coincide with the positions of the finger tips when V is minimized ($= V_{\min}$). Therefore, we derive the closed loop dynamics shown in (14) to (16) and V in (23) for an arbitrary polyhedral object.

For the multi-fingered hand-arm system:

$$\begin{aligned}
&\boldsymbol{H}\ddot{\boldsymbol{q}} + \left\{\frac{1}{2}\dot{\boldsymbol{H}} + \boldsymbol{S} + \boldsymbol{C}\right\}\dot{\boldsymbol{q}} \\
&\quad + \sum_{i=1}^{N}\left(\acute{N}_{Zi}\boldsymbol{J}_{0i}^{\mathrm{T}} - \Delta r_i\lambda_{iZ}\cos\theta_{si}\boldsymbol{J}_{\Omega i}^{\mathrm{T}}\right)\boldsymbol{r}_X \\
&\quad + \sum_{i=1}^{N}\left(\Delta r_i\lambda_{iX}\boldsymbol{J}_{\Omega i}^{\mathrm{T}} - \lambda_{iZ}\boldsymbol{J}_{0i}^{\mathrm{T}}\right)\boldsymbol{r}_Y \\
&\quad + \sum_{i=1}^{N}\left(-N_{Zi}\boldsymbol{J}_{0i}^{\mathrm{T}} - \Delta r_i\lambda_{iZ}\sin\theta_{si}\boldsymbol{J}_{\Omega i}^{\mathrm{T}}\right)\boldsymbol{r}_Z \\
&\quad - A\sum_{i=1}^{N}\left\{\left(\sum_{j=1}^{N}\acute{N}_{Wj} - N\acute{N}_{Wi}\right)\boldsymbol{J}_{0i}^{\mathrm{T}}\right\}\boldsymbol{r}_X \\
&\quad - A\sum_{i=1}^{N}\left\{\left(\sum_{j=1}^{N}Z_j - NZ_i\right)\boldsymbol{J}_{0i}^{\mathrm{T}}\right\}\boldsymbol{r}_Y \\
&\quad - A\sum_{i=1}^{N}\left\{\left(\sum_{j=1}^{N}N_{Wj} - NN_{Wi}\right)\boldsymbol{J}_{0i}^{\mathrm{T}}\right\}\boldsymbol{r}_Z \\
&\quad = \ 0,
\end{aligned} \tag{32}$$

For the object:

$$\boldsymbol{M}\ddot{\boldsymbol{x}} + \sum_{i=1}^{N}\left(-\acute{N}_{Zi}\boldsymbol{r}_X + \lambda_{iZ}\boldsymbol{r}_Y + N_{Zi}\boldsymbol{r}_Z\right) = 0 \tag{33}$$

$$\begin{aligned}
&\boldsymbol{I}\dot{\boldsymbol{\omega}} + \left\{\frac{1}{2}\dot{\boldsymbol{I}} + \boldsymbol{S}\right\}\boldsymbol{\omega} + \sum_{i=1}^{N}\left(-N_{Yi}\lambda_{iZ} - \acute{N}_{Xi}Z_i\right)\boldsymbol{r}_X \\
&\quad + \sum_{i=1}^{N}\left(f_iX_i + \lambda_{iX}Y_i\right)\boldsymbol{r}_Y \\
&\quad + \sum_{i=1}^{N}\left(-\acute{N}_{Yi}\lambda_{iZ} + N_{Xi}Z_i\right)\boldsymbol{r}_Z = 0,
\end{aligned} \tag{34}$$

where

$$\left[\begin{array}{l}
\theta_1 = 0 \\
\theta_i = \cos^{-1}\left(\boldsymbol{C}_{(i-1)Y}^{\mathrm{T}}\boldsymbol{C}_{iY}\right) \quad (i = 2, 3, ..., N) \\
\theta_{si} = \sum_{h=1}^{i}\theta_h \\
\boldsymbol{R}_{Ci} = \boldsymbol{R}^{-j\theta_{si}}\boldsymbol{R}^{-i\frac{\pi}{2}} \\
D_i = Y_i + \Delta r_i \\
N_{Wi} = X_i\sin\theta_{si} + D_i\cos\theta_{si} \\
\acute{N}_{Wi} = X_i\cos\theta_{si} - D_i\sin\theta_{si} \\
N_{Xi} = f_i\sin\theta_{si} + \lambda_{iX}\cos\theta_{si} \\
\acute{N}_{Xi} = f_i\cos\theta_{si} - \lambda_{iX}\sin\theta_{si} \\
N_{Yi} = Y_i\cos\theta_{si} + X_i\sin\theta_{si} \\
\acute{N}_{Yi} = Y_i\sin\theta_{si} - X_i\cos\theta_{si} \\
N_{Zi} = f_i\cos\theta_{si} + \lambda_{iX}\sin\theta_{si} \\
\acute{N}_{Zi} = f_i\sin\theta_{si} - \lambda_{iX}\cos\theta_{si},
\end{array}\right. \tag{35}$$

where Y_i is the distance from the center of the object mass $O_{c.m.}$ to the surface. From (32), (33) and (34), the scalar function V is given as follows:

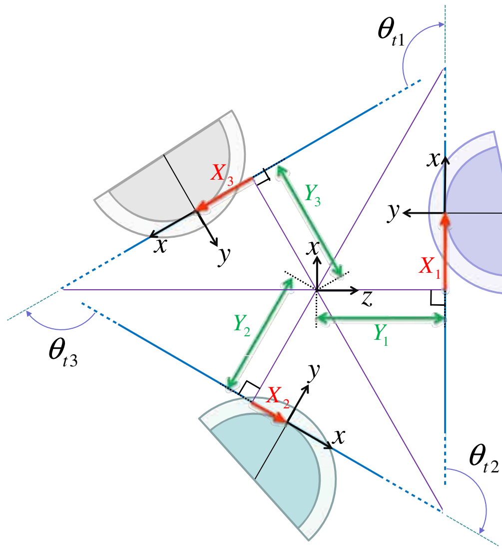

Fig. 3. Cross-section view of polygonal column

$$
\begin{aligned}
V = A\Big[&\left(X_1^2 + X_2^2 + \dots + X_N^2\right) + \left(D_1^2 + D_2^2 + \dots + D_N^2\right) \\
&- \{(D_1X_2 - X_1D_2)\sin\theta_{t2} + (D_2X_3 - X_2D_3)\sin\theta_{t3} \\
&\qquad + \dots + (D_NX_1 - X_ND_1)\sin\theta_{t1}\} \\
&- \{(X_1X_2 + D_1D_2)\cos\theta_{t2} + (X_2X_3 + D_2D_3)\cos\theta_{t3} \\
&\qquad + \dots + (X_NX_1 + D_ND_1)\cos\theta_{t1}\}\Big] \\
&+ \frac{A}{2}\Big\{(Z_1 - Z_2)^2 + (Z_2 - Z_3)^2 \\
&\qquad + \dots + (Z_N - Z_1)^2\Big\}, \qquad (36)
\end{aligned}
$$

where

$$\theta_{ti} = \theta_{si} - \theta_{s(i-1)} \quad (i \neq 1) \qquad (37)$$

$$\theta_{ti} = \theta_{si} - \theta_{sN} \quad (i = 1). \qquad (38)$$

θ_{ti} is the external angle of the polygon parallel to the base of the object (see Fig. 3). One of the prerequisite for the minimum value of V is

$$Z_1 = Z_2 = \dots = Z_N. \qquad (39)$$

In the case that the grasped object has arbitrary polyhedral shape, X_i can be considered as an index for evaluating the stability of the system from the physical perspective. In fact, stable grasping is realized if X_i is inside of each contact surface when V is minimized to $V_{\min}$, that is to say, the final state of the system is stable in the physical viewpoint. Equation (36) has three parameters X_i, D_i and θ_{ti}. As an example, we show the relation between X_i and θ_{ti} in Table I and the relation between X_i and D_i for $V_{\min}$ in the case that the object is a triangle pole, where the size of the triangle pole is normalized by the cross-section area S. Table II shows the relation between X_i and the radius of each finger tip r_i for $V_{\min}$ in order to show the relation between X_i and D_i for $V_{\min}$. In Table I and II, "IN" (see Fig. 4) means a case of success in which all the centers of the contact areas are inside of the object surface at the final state, and "OUT" (see Fig. 5) means a case of failure in which at least one of the centers of the contact areas is outside of the object surfaces at the final state. Table I and II show that the shape of the grasped object and the radius of each finger tip determine whether a stable grasping is realized or not at the final state. From these considerations, we can say that initial positions of the finger tips are valid for stable grasping if the initial positions are close to the position obtained when V is minimized to $V_{\min}$. Therefore, $V_{\min}$, the minimum value of the scalar function V, can be used as an index for evaluating the possibility of stable grasping.

TABLE I

RELATIONSHIP BETWEEN θ_{ti} AND X_i

	θ_{t1}[rad]	θ_{t2}[rad]	θ_{t3}[rad]	X_1[m]	X_2[m]	X_3[m]	
A	2.84	2.84	0.60	0.00	-0.0601	0.0601	IN
B	2.54	2.54	1.20	0.00	-0.0122	0.0122	IN
C	2.24	2.24	1.80	0.00	-0.0094	0.0094	IN
D	1.94	1.94	2.40	0.00	0.0190	-0.0190	IN
E	1.64	1.64	3.00	0.00	0.1137	-0.1137	OUT

$(r_j = 0.03\,[\mathrm{m}]\,, \Delta r_{\min} = 0.02\,[\mathrm{m}]\,, S = 6.38 \times 10^3\,[\mathrm{m}^2])$

TABLE II

RELATIONSHIP BETWEEN r_i AND X_i

	r[m]	$\Delta r_{\min}$[m]	X_1[m]	X_2[m]	X_3[m]	
F	0.030	0.020	0.00	0.0504	-0.0504	IN
G	0.050	0.040	0.00	0.0605	-0.0605	IN
H	0.070	0.060	0.00	0.0705	-0.0705	OUT

$((\theta_{t1}, \theta_{t2}, \theta_{t3}) = (1.79, 1.79, 2.70)\,[\mathrm{rad}], S = 6.38 \times 10^3\,[\mathrm{m}^2])$

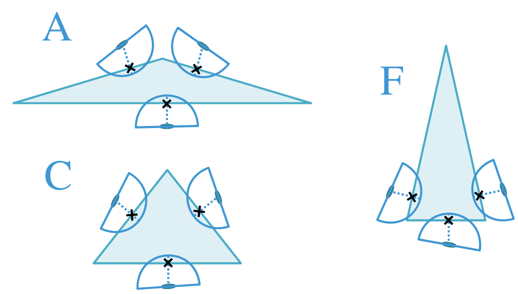

Fig. 4. Sample case of "IN" as shown in Table I (A, C) and II (F). IN : The case of success in which all the centers of the contact areas are inside of the object surfaces at the final state $(V = V_{\min})$

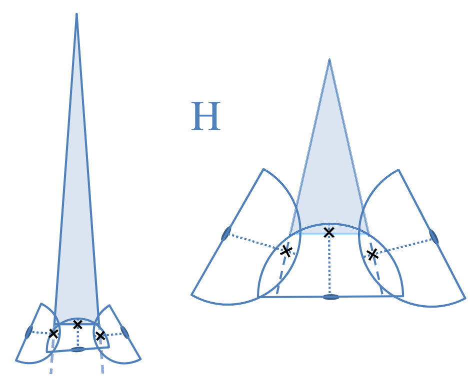

Fig. 5. Sample case of "OUT" as shown in Table I (E) and II (H). OUT : The case of failure in which at least one of the centers of the contact areas is outside of the object surfaces at the final state $(V = V_{\min})$

V. NUMERICAL SIMULATION

We conduct numerical simulations for verifying the proposed approach. The parameters of the triple-fingered hand-arm system and the object in numerical simulation are shown

TABLE III

PHYSICAL PARAMETERS

Triple-fingered hand-arm system

1^{st} link length l_{a1}	1.300[m]		
2^{nd} link length l_{a2}	1.000[m]		
3^{rd} link length l_{a3}	0.175[m]		
1^{st} link length l_{i1}	0.300[m]		
2^{nd} link length l_{i2}	0.200[m]		
1^{st} mass m_{a1}	1.300[kg]	1^{st} mass center l_{ga1}	0.650[m]
2^{nd} mass m_{a2}	1.000[kg]	2^{nd} mass center l_{ga2}	0.500[m]
3^{rd} mass m_{a3}	0.400[kg]	3^{rd} mass center l_{ga3}	0.0875[m]
1^{st} mass m_{i1}	0.250[m]	1^{st} mass center l_{gi1}	0.150[m]
2^{nd} mass m_{i2}	0.150[m]	2^{nd} mass center l_{gi2}	0.100[m]
1^{st} Inertia $\boldsymbol{I}_{a1}$	$\mathrm{diag}(7.453, 7.453, 0.260)\times 10^{-1}$[kg·m^2]		
2^{nd} Inertia $\boldsymbol{I}_{a2}$	$\mathrm{diag}(3.397, 3.397, 0.128)\times 10^{-1}$[kg·m^2]		
3^{rd} Inertia $\boldsymbol{I}_{a3}$	$\mathrm{diag}(0.291, 0.291, 0.500)\times 10^{-1}$[kg·m^2]		
1^{st} Inertia $\boldsymbol{I}_{i1}$	$\mathrm{diag}(7.725, 7.725, 0.450)\times 10^{-3}$[kg·m^2]		
2^{nd} Inertia $\boldsymbol{I}_{i2}$	$\mathrm{diag}(2.060, 2.060, 0.120)\times 10^{-3}$[kg·m^2]		
Radius of fingertip r_i	0.070[m]		
Stiffness coefficient k_i	1.000×10^5[N/m^2]		
Damping function ξ_i	$1.000\times\left(r_i^2-\Delta r_i^2\right)\pi$[Ns/m^2]		

Object

Mass m	0.037[kg]
(Y_1, Y_2, Y_3)	(0.092, 0.048, 0.048)[m]
$(\theta_{t1}, \theta_{t2}, \theta_{t3})$	(1.833, 1.833, 2.618)[rad]
Inertia $\boldsymbol{I}$	$\mathrm{diag}\,(1.273, 0.193, 1.148)\times 10^{-3}$[kg · m^2]

TABLE IV

DESIRED GRASPING FORCE AND GAINS

f_d	1.0[N]
$\boldsymbol{C}_a$	$\mathrm{diag}(3.080, 2.065, 2.483, 0.768, 0.487)\times 10^{-2}$[Ns·m/rad]
$\boldsymbol{C}_i$	$\mathrm{diag}(0.164, 0.177, 0.064)\times 10^{-2}$[Ns·m/rad]

TABLE V

INITIAL CONDITION

$\dot{\boldsymbol{q}}$	$\mathbf{0}$[rad/s]
$\boldsymbol{q}_a$	$(-0.262, -1.571, 2.094, 0.785, 0.000)^{\mathrm{T}}$ [rad]
$\boldsymbol{q}_{01}$	$(0.000, -0.663, 1.934)^{\mathrm{T}}\times 10^{-2}$[rad]
$\boldsymbol{q}_{02}$	$(-0.262, -0.705, 2.185)^{\mathrm{T}}\times 10^{-2}$[rad]
$\boldsymbol{q}_{03}$	$(0.262, -0.705, 2.185)^{\mathrm{T}}\times 10^{-2}$[rad]
$\dot{\boldsymbol{x}}$	$\mathbf{0}$[m/s]
$\boldsymbol{x}$	$(0.000, 0.600, 0.800)^{\mathrm{T}}$ [m]
$\boldsymbol{\omega}$	$\mathbf{0}$[rad/s]
$\boldsymbol{R}$	$\begin{bmatrix} 1 & 0 & 0 \\ 0 & 1 & 0 \\ 0 & 0 & 1 \end{bmatrix}$

in Table III. Table IV and V show the desired grasping force and gains, and the initial condition, respectively. The results of the grasping simulation are depicted in Figs. 6–10. From Fig. 6 which indicates X_i and Z_i, we can see that X_i converges to which V satisfies $V_{\min}$, and thus, the condition of (39) is satisfied. In addition, X_i and Z_i converge to the values which satisfy the conditions for $V_{\min}$. From these results, we can conclude that the analysis of $V_{\min}$ is useful and it can be regarded as one of the index for evaluating whether stable grasping is realized or not. This is also effective for evaluating the initial positions of each finger tips. Figures 7 and 8 show the elements of $\boldsymbol{\Delta}\lambda_\infty$ converges to zero. It indicates that the sum of external force applied to the system and the object converges to zero. The results illustrate that the dynamic force/torque equibilium condition for immobilization of the object is satisfied. Figures 9 and 10 show $\dot{\boldsymbol{q}}$, $\dot{\boldsymbol{x}}$ and $\boldsymbol{\omega}$ and we can confirm that the velocities of the overall system converge to zero.

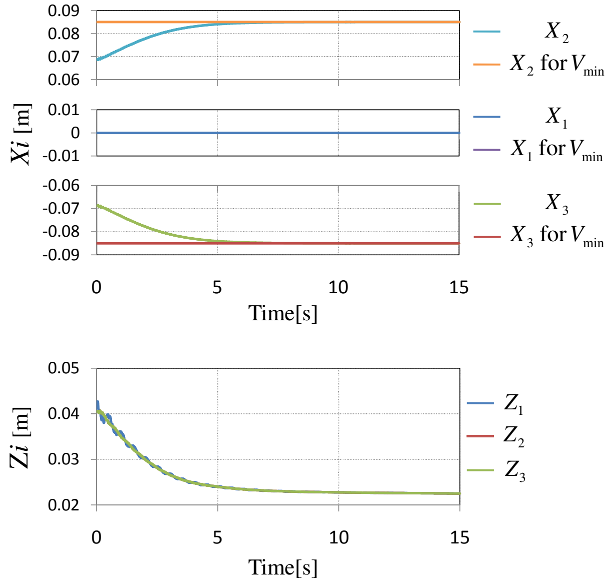

Fig. 6. History of X_i reach to X_i for $V_{\min}$ and history of Z_i satisfies (39)

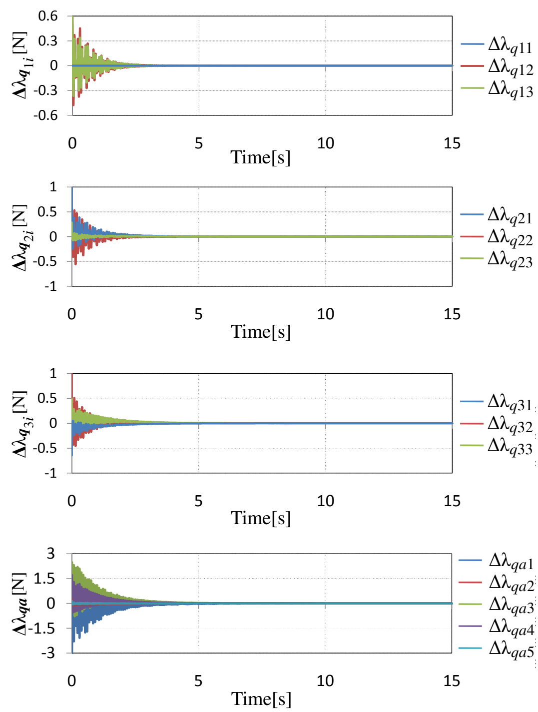

Fig. 7. External force applied to the system convergence to zero

VI. CONCLUSION

This paper presented the novel stable grasping method for an arbitrary polyhedral object by a multi-fingered hand-arm system. Firstly, the nonholonomic constraints of rolling contact were formulated, and the conditions to realize the stable grasping was derived from the stability analysis of the overall system. Additionally, a new index obtained by the scalar function $V_{\min}$ was proposed for evaluating the possibility of stable grasping. This possibility depends only

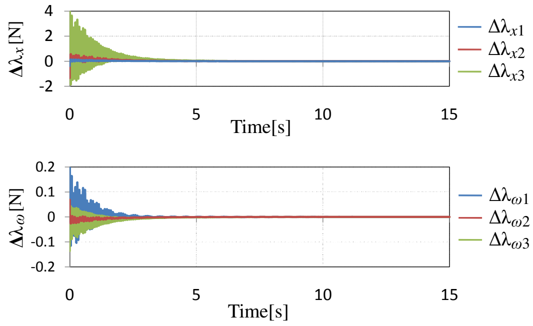

Fig. 8. External force applied to the object convergence to zero

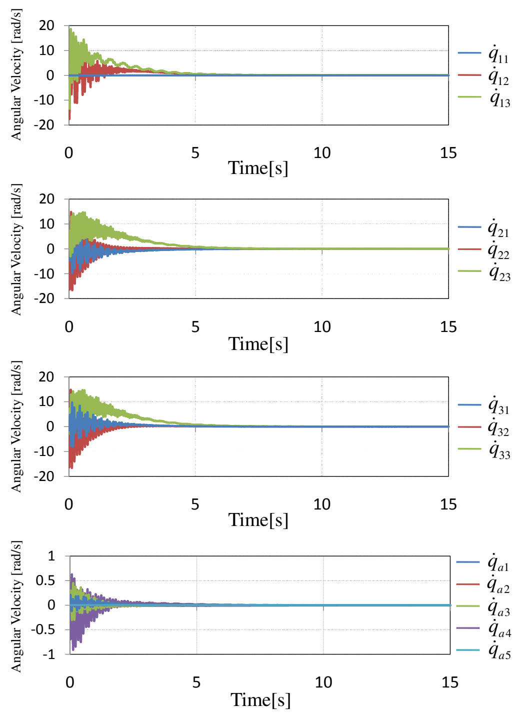

Fig. 9. History of joint angler velocity of arm and each finger

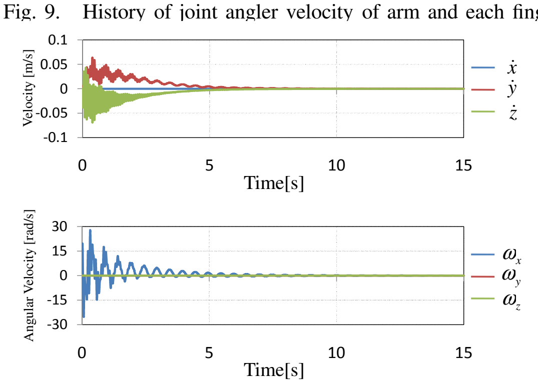

Fig. 10. History of translational and rotational velocity of grasped object

on the shape of potential function V, and it does not depend on initial contact positions and soft finger contact model. The usefulness of the proposed index was verified through numerical simulations. This means that the proposed method realizes stable grasping regardless of any external sensing and that the preshaping of the hand-arm system for approaching to the object is important to realize stable grasping.

Currently, the position and orientation of the object are not specified explicitly. However, it would be easily possible to control the position and orientation of the grasped object by referring to the method proposed by Tahara *et al.* [17] and Bae *et al.* [18]. In the future works, we would like to perform some experiments to verify the usefulness of our proposed method. Furthermore, we will expand the proposed control scheme for an object with curved surfaces.

Acknowledgment

This work was partially supported by ”the Kyushu University Research Superstar Program (SSP)”, based on the budget of Kyushu University allocated under President’s initiative.

References

[1] M. R. Cutkosky, *Grasping and Fine Manipulation*, Kluwer Academic, Dordrecht, Netherlands; 1985.

[2] R. M. Murray, Z. Li and S. S. Sastry, *Mathematical Introduction to Robotic Manipulation*, CRC Press, Boca Raton; 1994.

[3] K. B. Shimoga, “Robot grasp synthesis algorithms: A survey,” *Int. J. Robotics Research*, vol. 15, no. 3, pp. 230–266, 1996.

[4] A. M. Okamura, N. Smaby and M. R. Cutkosky, “An overview of dexterous manipulation,” *Proc. of the 2000 IEEE Int. Conf. Robot. Automat.*, pp. 255–262, SanFrancisco, CA, 2000.

[5] A. Bicchi, “Hands for dexterous manipulation and robust grasping: A difficult road towards simplicity,” *IEEE Trans. Robot. Automat.*, vol. 16, no. 6, pp. 652–662, 2000.

[6] D. Montana, “The kinematics of contact and grasp,” *Int. J. Robot. Res.*, vol.7, no. 3, pp. 17-32, 1988.

[7] A. Cole, J. Hauser and S. Satry, “Kinematics and control of multifingered hands with rolling contacts,” *IEEE Trans. Automat. Contr.*, vol. 34, no. 4, pp. 398–404, 1989.

[8] L. Han and J. Trincle, “Dexterous manipulation by rolling and finger gaiting,” *Proc. IEEE Int. Conf. Robot. Automat.*, vol. 1, pp. 730–735, 1998.

[9] K. Harada, M. Kaneko and T. Tsuji, “Rolling based manipulation for multiple objects,” *Proc. IEEE Int. Conf. Robot. Automat.*, vol. 4, pp. 3887–3894. 2000.

[10] Y. Yokokohji, M. Sakamoto and T. Yoshikawa, “Vision-aided object manipulation by a multifingered hand with soft fingertips,” *Proc. IEEE Int. Conf. Robot. Automat.*, pp. 3202–3208, 1999.

[11] D. Gunji, Y. Mizoguchi, S. Teshigawara, A. Ming, A. Namiki, M. Ishikawa and M. Shimojo, “Grasping force control of multi-fingered robot hand based on slip detection using sensor,” *IEEE Int. Conf. Robot. Automat.*, pp. 2605–2610, Pasadena, CA, 2008.

[12] T. Takahashi, T. Tsuboi, T. Kishida, Y. Kawanami, S. Shimizu, M. Iribe, T. Fukushima and M. Fujita, “Adaptive grasping by multi fingered hand with tactile sensor based on robust force and position control,” *IEEE Int. Conf. Robot. Automat.*, pp. 264–271, Pasadena, CA, 2008.

[13] T. Wimböck, C. Ott, and G. Hirzinger, “Passivity-based Object-Level Impedance Control for a Multifingered Hand,” *Proc. of the 2006 IEEE/RSJ on Intelligent Robots and Systems*, pp. 4621–4627, Beijing, Chine, 2006.

[14] S. Arimoto, P.T.A. Nguyen, H.-Y. Han and Z. Doulgeri, “Dynamics and control of a set of dual fingers with soft tips,” *Robotica*, vol. 18, no. 1, pp. 71–80, 2000.

[15] S. Arimoto, “A differential-geometric approach for 2-D and 3-D object grasping and manipulation,” *Annual Review in Control*, Vol. 31, pp. 189–209, 2007.

[16] M. Yoshida, S. Arimoto and J.-H. Bae, “Blind grasp and manipulation of a rigid object by a pair of robot fingers with soft tips,” *Proc. of the 2007 IEEE Int. Conf. Robot. Automat.*, pp. 4707–4714, Roma, Italy, 2007.

[17] K. Tahara, S. Arimoto and M. Yoshida, “Dynamic object grasping by a triple-fingered robotic hand,” *2008 IEEE/RSJ Int. Conf. on Intelligent Robots and Systems.*, pp. 2685–2690, Nice, France, 2008.

[18] J.-H. Bae, S. Arimoto, R. Ozawa, M. Sekimoto and M. Yoshida, “A unified control scheme for a whole robotic arm-fingers system in grasping and manipulation”, *Proc. of the 2006 IEEE Int. Conf. Robot. Automat.*, pp. 2131–2136, Orlando, Florida, 2006.